BMC Microbiology

RESEARCH

Open Access

Fecal microbiota transplantation mitigates postdieting weight regain in mice by modulating the gut-liver axis

Hong Cao[1,2,3,4], Jiangwei Xu[1,2,3,4], Han Wang[1,2,3,4], Wanya Yi[1,2,3,4], Dandan Yang[1,2,3,4], Ju Yang[1,2,3,4], Jing Sun[1,2,3,4], Yingyu Wang[1,2,3,4], Feng Zhang[1,2,3,4], Jiai Yan[1,2,3,4*] and Dan Li[1,2,3,4*]

Abstract

Background Dysbiosis of the microbiome is strongly associated with weight rebound after dieting. However, the interactions between the host and microbiome and their relevance to the pathogenesis of post-diet weight rebound remain unclear.

Purpose This study aimed to evaluate the effects of fecal microbiota transplantation (FMT) on post-diet weight regain and to investigate the underlying mechanisms by which FMT inhibits weight regain.

Methods FMT was administered once daily to mice for 5 weeks. Gas chromatography tandem mass spectrometry was employed to analyze short-chain fatty acid levels in serum, ultrahigh-performance liquid chromatography tandem mass spectrometry was utilized for analyzing hepatic lipid metabolites, and shotgun metagenomic sequencing was applied to examine the intestinal microbiome.

Results FMT reduced weight regain and prevented lipid accumulation in both liver and adipose tissue while also improving glucose intolerance in mice. Furthermore, FMT increased the abundance of Enterorhabdus caecimuris and decreased the abundances of Burkholderiales, Sutterellaceae, Turicimonas muris, Bacteroides stercorirosoris, and Acetivibrio ethanolgignens within the gut microbiota. Additionally, elevated propionic acid levels and significant alterations in hepatic lipid metabolites were observed following FMT administration.

Conclusions Our findings demonstrate that FMT effectively mitigates post-diet weight regain and associated complications. These effects are mediated through interactions between the gut microbiota and the liver via the gut-propionic acid-liver axis.

Clinical trial number Not applicable.

Keywords Weight regain, Fecal microbiota transplantation, Lipid metabolism, Gut-liver axis, Propionic acid

*Correspondence:
Jiai Yan
yanjiai@jiangnan.edu.cn
Dan Li
danliyyh@jiangnan.edu.cn

[1]Department of Nutrition, Affiliated Hospital of Jiangnan University, Wuxi, China
[2]Wuxi School of Medicine, Jiangnan University, Wuxi, China
[3]Institute of Future Food Technology, JITRI, Yixing 214200, China
[4]Clinical Assessment Center of Functional Food, Affiliated Hospital of Jiangnan University, Wuxi, China

© The Author(s) 2025. **Open Access** This article is licensed under a Creative Commons Attribution-NonCommercial-NoDerivatives 4.0 International License, which permits any non-commercial use, sharing, distribution and reproduction in any medium or format, as long as you give appropriate credit to the original author(s) and the source, provide a link to the Creative Commons licence, and indicate if you modified the licensed material. You do not have permission under this licence to share adapted material derived from this article or parts of it. The images or other third party material in this article are included in the article's Creative Commons licence, unless indicated otherwise in a credit line to the material. If material is not included in the article's Creative Commons licence and your intended use is not permitted by statutory regulation or exceeds the permitted use, you will need to obtain permission directly from the copyright holder. To view a copy of this licence, visit http://creativecommons.org/licenses/by-nc-nd/4.0/.

Introduction

Over the past century, the prevalence of obesity has increased worldwide [1–3]. Obesity is recognized as a significant risk factor for numerous severe diseases, including diabetes mellitus, nonalcoholic liver disease, cardiovascular disease, hypertension and stroke, and certain forms of cancer, all of which can negatively affect life expectancy, quality of life, and healthcare costs [4, 5]. Despite ongoing efforts in the medical and scientific fields, strategies aimed at preventing and treating obesity at both individual and population levels have not achieved long-term success. Although dietary restrictions can effectively induce weight loss, maintaining that weight loss is challenging. In fact, the majority of individuals who lose weight eventually regain it over time [6]. The impact of genetic factors on postdieting weight regain is believed to be minimal [7], but the non-genetic factors contributing to this recurrent obesity phenomenon remain unclear. Given the high prevalence of dieting among young adults, adolescents, and even children, further scientific investigations are warranted to elucidate the mechanisms underlying weight cycling-induced obesity [8].

The pivotal role of the microbiota in metabolic health and obesity has generated significant interest in recent decades. The gut microbiota is considered an organ capable of performing intricate functions and producing numerous metabolites that can interact with the host through direct or indirect mechanisms, thereby influencing host metabolism [9]. Alterations in the microbiome have been suggested to contribute to the development of obesity by modulating circulating metabolites [10]. Moreover, variations in dietary lipids can rapidly modify the composition and function of the microbiome [11, 12].

Strategies targeting the gut microbiome have gained increasing attention from researchers, with fecal microbiota transplantation (FMT) being considered a therapeutic option for restoring alterations in the gut microbiome associated with obesity [13]. Given the high prevalence of obesity and mounting evidence supporting the crucial role of the gut microbiome in post-dieting weight regain [14], our objective was to investigate the therapeutic potential of FMT in mitigating weight regain after dieting.

In this study, we employed mouse models of weight loss and recurrent obesity to investigate the effects of autologous and allogeneic FMT on obesity and post-dieting weight regain. FMT was administered during three different phases: mice were exposed to a primary high-fat diet (HFD), a normal diet (ND), and a second HFD. Our findings revealed that autologous and allogeneic FMT resulted in a reduction in weight regain and alleviation of exacerbated metabolic complications following weight cycling, but only during re-exposure to a HFD. These FMT interventions modulated hepatic lipid metabolism and energy homeostasis, altered the composition of the gut microbiota, and increased the levels of propionic acid.

Table 1 Normal and high-fat diet formulas

ND			HFD		
Ingredient	gm	kcal	Ingredient	gm	kcal
Casein	200	800	Casein	200	800
DL-Methionine	3	12	L-Cystine	3	12
Corn starch	150	600	Corn starch	0	0
Sucrose	500	2000	Maltodextrin	125	500
Cellulose, BW200	50	0	Sucrose	72.8	291.2
Core Oil	50	450	Cellulose, BW200	50	0
Mineral Mix. S10001	35	0	Soybean Oil	25	225
Vitamin Mix. V10001	10	40	Lard	245	2250
Choline Bitartrate	2	0	Mineral Mix. S10026B	50	0
			Vitamin Mix. V10001C	1	4
			Choline Bitartrate	2	0

Materials and methods

Mouse experiment

Fifty-four male C57BL/6JGpt mice (4 weeks old) were purchased from GemPharmatech Co., Ltd. (Jiangsu, China) and used in this study after acclimatization for one week. The mice were housed in a specific-pathogen-free animal facility with controlled temperature (25 °C) and humidity and a 12 h–12 h light–dark cycle. The animals had free access to food (Jiangsu Synergy Pharmaceutical & Biological Engineering Co., Ltd, specific formulations are listed in Table 1.) and water throughout the duration of the experiment. All animal experiments were conducted in accordance with ethical regulations and protocols approved by the Institutional Animal Care and Use Committee of Jiangnan University. These mice were randomly divided into nine groups of six mice each.: the ND group, the HFD group, a mouse recurrent obesity model group (cycHFD) established by subjecting the mice to five weeks of HFD(first cycle) followed by five weeks of ND(second cycle) and then five weeks of HFD(third cycle), the first cycle of autologous FMT under cycHFD (AutA), the second cycle of autologous FMT under cycHFD (AutB), the third cycle of autologous FMT under cycHFD (AutC), the first cycle of heterologous FMT under cycHFD (AllA), the second cycle of heterologous FMT under cycHFD (AllB), and the third cycle of heterologous FMT under cycHFD (AllC). The experimental design is illustrated in Fig. 1a. The body weights of the mice were measured once a week. After the experiment, the mice were anesthetized by inhaling 2% isoflurane, and blood was collected by eyeball blood collection. When the blood was drained out, the mice were killed by dislocating, and liver, adipocytes, and intestinal cecal contents were collected for further analysis.

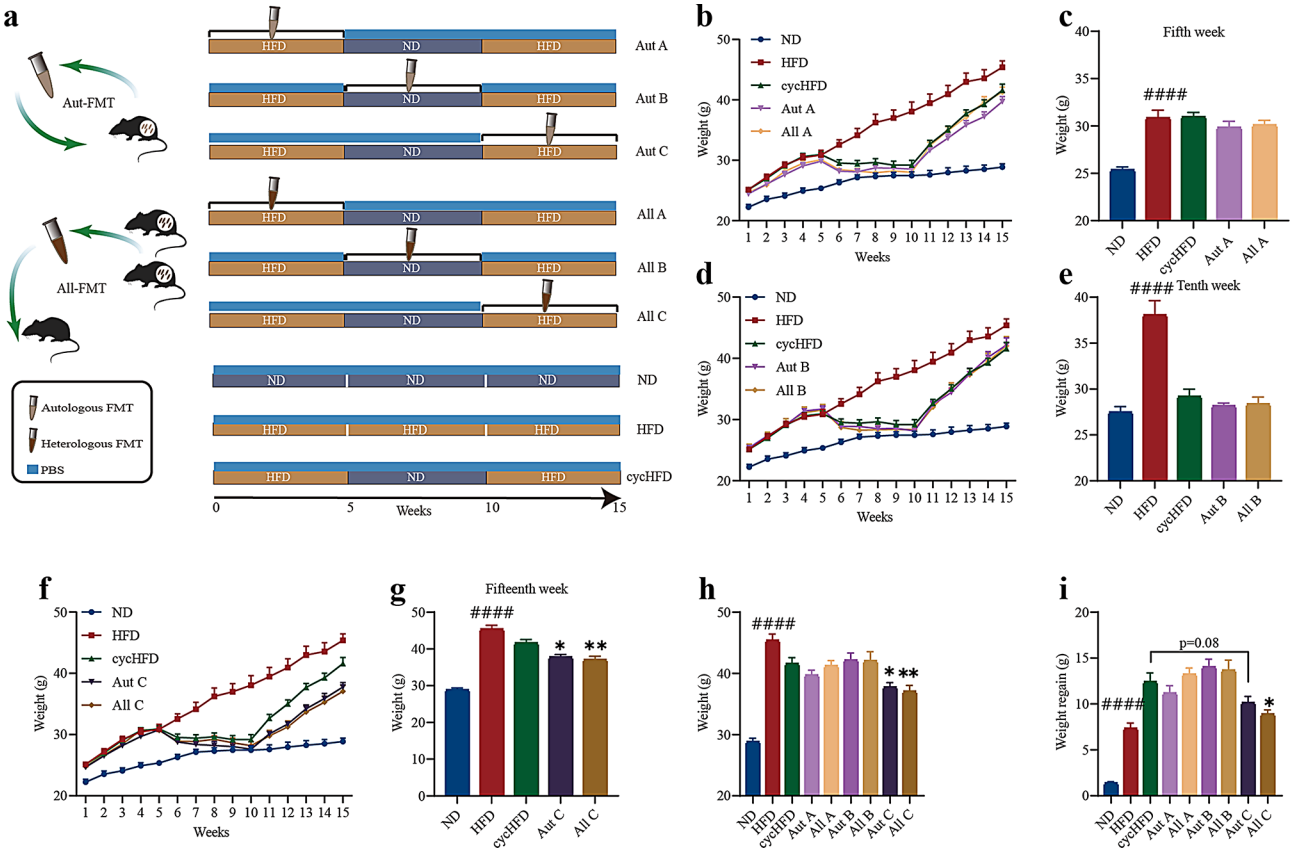

Fig. 1 Effects of FMT on postdieting weight regain. **a**, Schematic illustration of the experimental groups of mice ($n=6$ in each group) and the experimental procedures. **b**-**c**, Weight curves (**b**) and body weights at week 5 (**c**) in the AutA, AllA and control groups. **d**-**e**, Weight curves (**d**) and body weights at week 10 (**e**) in the AutB, AllB and control groups. **f**-**g**, Weight curves (**f**) and body weights at week 15 (**g**) in the AutC, AllC and control groups. **h**-**i**, Body weight (**h**) and weight regain quantification (**i**) in all groups at the end of the study. $n=6$ per group. The data are presented as the mean ± s.e.m. ###$P<0.001$, ####$P<0.0001$ vs. the ND group; *$P<0.05$, **$P<0.01$ vs. the cycHFD group

Preparation of fecal transplant material

The faecal material was collected and prepared according to an established protocol [15]. Faeces were collected one week prior to the experimental intervention, during which the donor mice were maintained on a ND and had free access to food and water. Faeces were collected at specific time points and immediately preserved in phosphate buffer solution (PBS) containing 20% glycerol and frozen to -80 °C. During the FMT intervention phase, faeces were resuspended in 1 ml of PBS solution. The solution was vigorously mixed for 30 s using a benchtop vortex mixer (VM-02U, Suzhou Jimei Electronics Co., Ltd.) and then centrifuged at 800 × g for 3 min. The supernatant was collected as transplantation material. Recipient mice received autologous or allogeneic graft material orally every day. Each mouse in the AutA, AutB, and AutC groups received its own feces, while recipient mice in the AllA, AllB, and AllC groups were transplanted with a mixture of feces collected from all mice in their respective groups. All feces were collected prior to the intervention.

Metabolic parameters

The energy consumption and energy expenditure of the mice were assessed using a Comprehensive Laboratory Animal Monitoring System (CLAMS-16 MR/CIS-16 MR, Columbus Instruments, USA); The metabolic cages were placed within an environment-controlled facility at Jiangnan University. Prior to data collection, mice are individually housed and acclimatized in a metabolic chamber for 24 h. Afterwards, each mouse is continuously monitored for 48 h under alternating cycles of 12 h of light and 12 h of darkness. This allows for the quantitative analysis of food intake, CO_2 production, and O_2 consumption. During the assay period, the mice have unrestricted access to food and water, and the room temperature is maintained at 25 °C.

Oral glucose tolerance test

The mice (20 weeks old) underwent a 12 h fasting period, followed by oral administration of glucose (2 g/kg). Blood glucose levels were measured at 0, 15, 30, 60, 90 and 120 min after the glucose challenge using a Roche

ACCU-CHEK® Performa glucometer (Roche Diagnostics GmbH, Basel, Switzerland).

Micro-CT detection of fat volume

The mice were placed in a transparent plastic box and anesthetized using isoflurane (5% for induction, 1–2% for maintenance) mixed with oxygen (1 L/min). Once adequately anesthetized, the animals were placed in a head holder within the Micro-CT (quantum GXII, PE, Germany). The scanning parameters included a voltage of 90 kV, current of 80 μA, field of view of 86 mm, scanning time of 4 min, high-resolution mode selected for scanning, a 0.1 Cu filter employed during the acquisition process and a layer thickness of 172 μm.

ELISA

Serum samples were collected from the mice at the end of the experiment. Subsequently, assays were performed using ELISA kits for mouse IL-6 (CSB-E04639m; CUSABIO, Shanghai, China), mouse TNF-α (CSB-E04741m; CUSABIO, Shanghai, China), mouse leptin (H174-1-2; Nanjing JianCheng Bioengineering Institute) and mouse insulin (Cat # CEA448Mu; USCN Life Science Inc.) in accordance with the respective user manuals.

Biochemical evaluation

The levels of triglycerides (TGs), total cholesterol (TC), low-density lipoprotein cholesterol (LDL-C) and high-density lipoprotein cholesterol (HDL-C) were measured in the serum of the mice using an automatic biochemical analyzer (Beckman Coulter au 680; Beckman Coulter Corporation, America).

Histological analyses

Following fixation with 4% polyformaldehyde, the liver and brown adipose tissue were dehydrated and paraffin embedded. Subsequently, tissue Sect. (3 μm thick) were rehydrated and stained with hematoxylin-eosin (H&E) according to standard protocols. The resulting slides were then photographed under a microscope (Olympus, IX83, Japan) at a magnification of 40x.

Western blot analysis

Brown adipose tissue (BAT) and liver tissue were weighed and excised. Tissue samples were homogenized in RIPA buffer (P0013B; Beyotime) supplemented with protease inhibitors (P1005; Beyotime) and phosphatase inhibitors (P1086; Beyotime). Protein extracts were collected after centrifugation of the lysates (20 min, 12,000 rpm, 4 °C). Sample proteins (30 μg) were separated on an appropriate acrylamide gel and subsequently transferred onto a nitrocellulose membrane by electroblotting. Western blot analysis was performed using anti-uncoupling protein 1 (UCP1) (1:5000; ab209483; Abcam), anti-fatty acid synthase (FASN) (1:500; A21398; ABclonal) and anti-β-actin antibodies (1:8000; AF5003; Beyotime). The secondary antibody used was anti-rabbit IgG-HRP (1:10000; A0208; Beyotime). Image acquisition was performed using a Tennant 4800 fully automated chemiluminescence imager equipped with a high-resolution camera. Samples were exposed to a specific light source, and images were captured with appropriate settings to ensure a clear and accurate display of protein bands. Subsequently, the intensity of the bands was calculated using ImageJ software and normalized to the density of the β-actin bands.

Ultrahigh-performance liquid chromatography tandem mass spectrometry (UHPLC-MS) analysis of hepatic lipid metabolites

Lipid extraction was conducted following the Bligh and Dyer procedure as described previously [16]. The samples were analyzed using an EASY nLC 1200 ultrahigh-performance liquid chromatograph (UHPLC) (Thermo Fisher Scientific, Waltham, MA, USA) coupled with a Q Exactive mass spectrometer (Thermo Fisher Scientific, Waltham, MA, USA). The obtained lipid profiling data were analyzed using the online Metaboanalyst tool (www.metaboanalyst. ca.). Lipid species with a false discovery rate (FDR) < 0.05 and a fold change (FC) > 2.0 were considered significantly differentially abundant metabolites. KEGG pathway enrichment analysis was subsequently performed to predict the metabolic pathways associated with these differentially abundant metabolites.

Gas chromatography tandem mass spectrometry (GC–MS) analysis of short-chain fatty acids (SCFAs)

The SCFA standards were prepared with concentration gradients of 0.1, 0.5, 1, 5, 10, 20, 50, and 100 μg/mL. Then, the cecal contents (50 mg) were homogenized with phosphoric acid (50 μl) and ether (400 μl), with isocaproic acid serving as the internal standard. After vortexing (1 min), ultrasonication (5 min, 0 °C), and centrifugation (10 min, 12,000 rpm, at 4 °C), the supernatant was collected and filtered through a 0.22-μm microwell filter membrane. The analysis was performed using a GC/MS instrument equipped with an HP-FFAP capillary column (30 m× 0.25 mm× 0.25 μm) in a trace 1310 GC system.

High-purity helium gas (1 mL/min) was used as the carrier gas. The sample solution (1 μL) was injected in split mode at a 10:1 ratio and an injector temperature of 250 °C. The oven temperature was programmed as an initial temperature of 90 °C, followed by an increase to 120 °C at 10 °C/min, then to 150 °C at 5 °C/min, and finally, to 250 °C at 25 °C/min, where it was maintained for 2 min. The inlet temperature was 250 °C, the ion source temperature was 230 °C, the transfer line

temperature was 250 °C, and SIM modes were used with a collision energy of 70 eV.

Metagenomic analysis

The fecal samples were collected at the end of the experiment. Shotgun metagenomic sequencing analysis was performed on fecal samples from the AutC, AllC and cycHFD groups to evaluate the changes in the gut microbiota. Total microbial DNA was extracted from fecal samples using the E.Z.N.A.® Soil DNA Kit (Omega Bio-Tek, Norcross, GA, USA) according to the manufacturer's instructions. For paired-end library construction, genomic DNA was fragmented to an average size of approximately 300 bp. Illumina paired-end libraries were generated. Shallow shotgun sequencing was subsequently performed on the Illumina NovaSeq platform using a 2 × 150 bp paired-end protocol at Honsunbio Technology Co., Ltd. (Shanghai, China) with NovaSeq Reagent Kits (www.illumina.com). Quality control and preprocessing of the raw FASTQ reads were performed using fastp. Samples that passed strict quality control were included in the downstream analyses. Reads from the metagenomic dataset were assembled using Megahit (v1.1.2; https://github.com/voutcn/megahit). MetaGene (http://metagene.cb.k.u-tokyo.ac.jp/) was used to predict open reading frames (ORFs) from the assembled contigs and translate them into amino acids. The predicted genetic sequences of all the samples were clustered (parameters as follows: 95% identity and 90% coverage) using CD-HIT software (http://www.bioinformatics.org/cd-hit/) [17], and the longest gene of each class was taken as a representative sequence to construct a nonredundant gene catalog. The high-quality reads from each sample were mapped to the nonredundant gene catalog using SOAPaligner software (version 2.22, http://soap.genomics.org.cn/) [18], and the gene abundance was calculated. The sequences of the nonredundant gene catalog were aligned against the NCBI NR database for taxonomic annotation and against the KEGG database using Diamond (version 0.8.35, https://github.com/bbuchfink/diamond) for functional annotation.

Statistical analysis

The data are presented as medians or mean values ± standard errors of measurement for continuous variables based on their distributions. All the statistical analyses were performed using GraphPad Prism 9 software. The t test or Mann–Whitney U test was used to compare two groups for significant differences. We used one-way analysis of variance (ANOVA) for multiple comparisons involving more than two groups. (* $P < 0.05$, ** $P < 0.01$, *** $P < 0.001$).

To evaluate changes in microbial community composition and function, principal coordinates analysis (PCoA) was conducted using Bray–Curtis similarity matrices. A nonparametric Kruskal–Wallis test combined with pairwise Wilcoxon tests was applied to detect differences in the microbial community and functional diversity among the groups. Spearman's rank correlation coefficient was used to examine the relationships between the specific species and the functional terms (KEGG pathways and KO terms). P values were adjusted for multiple comparisons using the Benjamini–Hochberg method. A FDR and $p < 0.05$ were considered to indicate statistical significance unless otherwise stated.

Result

Effects of FMT on postdieting weight regain

To investigate the effect of fecal microbiota on weight regain after dieting and to determine the most effective intervention plan, the researchers conducted cycle diet experiments using mice. At each stage of the experiment, the mice were administered either fecal microbiota or vehicle (Fig. 1a). Consequently, the mice experienced a cycle of weight gain, weight loss and weight regain. During the first HFD and ND feeding periods, FMT had minimal effects on body weight, with no significant differences observed in subsequent weight regain among the AutA, AllA, AutB, AllB and cycHFD groups (Fig. 1b-e). Notably, during re-exposure to a HFD, a reduction in body weight (Fig. 1f, g) and a decrease in weight regain (-18.28% and − 28.36%, $p = 0.08$ and $p < 0.05$, respectively) (Fig. 1h, i) were observed in the AutC and AllC groups compared to those in the cycHFD group. These results indicate that FMT ameliorated postdieting weight regain in mice re-exposed to a HFD. Furthermore, allogeneic FMT exhibited better efficacy than autologous FMT. Therefore, we focused our analysis on the FMT-C (AutC and AllC) and cycHFD groups for further investigation.

The improvement in obesity-related complications

As expected, the cycHFD group developed exacerbated metabolic complications similar to those observed in the HFD group. Interestingly, the FMT-C groups were protected from these complications. The increases in serum levels of fasting plasma glucose (FPG) (Fig. 2a), insulin (Fig. 2b), triacylglycerol (TG) (Fig. 2p), and total cholesterol (TC) (Fig. 2q) were attenuated, and glucose tolerance improved (Fig. 2c, d) in the FMT-C groups compared to the cycHFD group. Additionally, body fat was reduced, as indicated by decreases in the volume (Fig. 2g-h) and weight (Fig. 2n-o) of subcutaneous and visceral fat tissues. Similarly, the lipid content in liver, and epididymal white adipose tissue was decreased, as demonstrated by H&E staining (Fig. 2i), an increased number of cells (Fig. 2j, l), decreased cell area (Fig. 2k, m), and reduced tissue TG levels (Fig. 2t, u). These findings suggest that FMT could improve weight regain-related

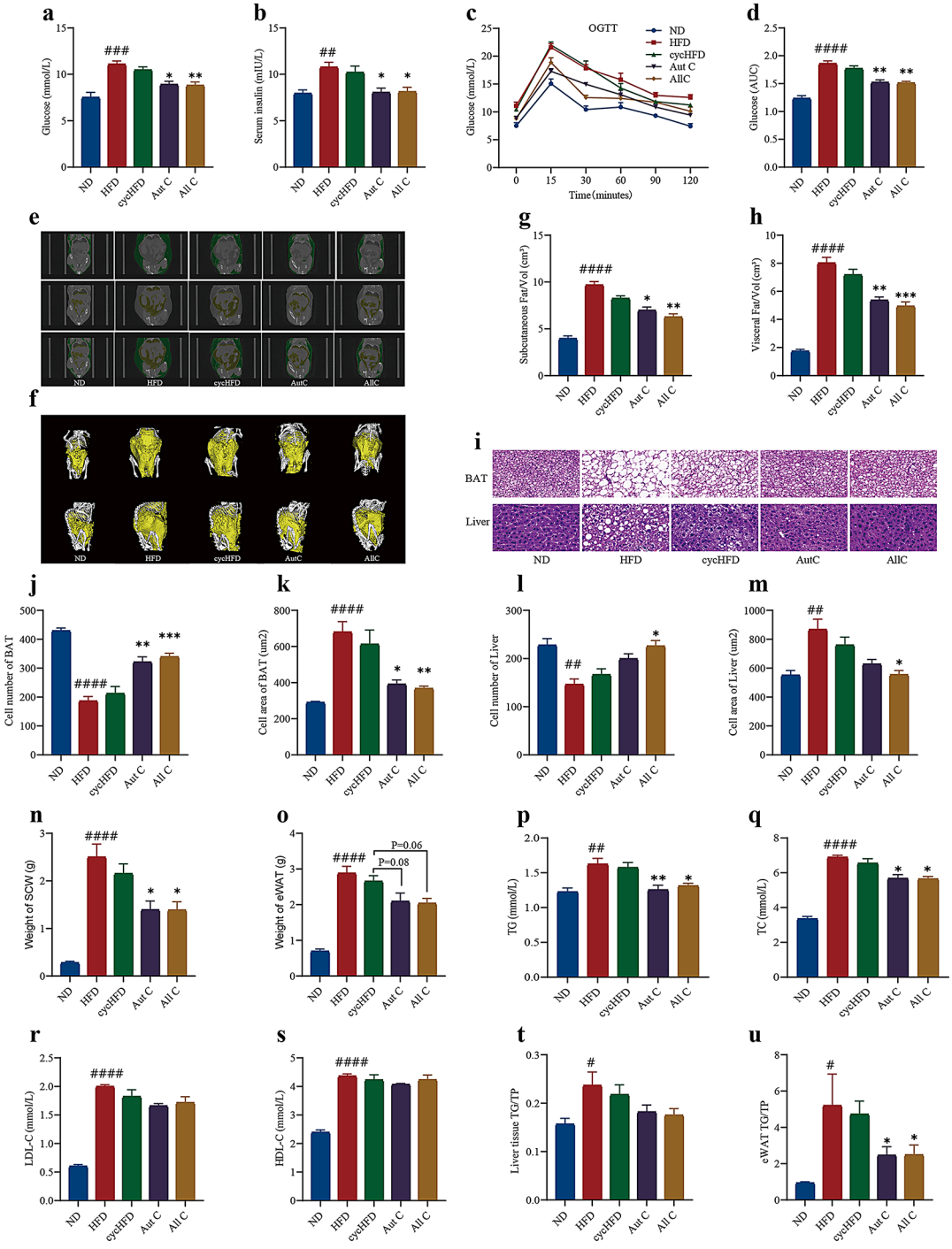

Fig. 2 The improvement in obesity-related complications. **a**-**h**, Fasting plasma glucose (**a**), serum insulin (**b**), oral glucose tolerance test (**c**), glucose quantification (**d**), representative CT scans (**e**), representative images of 3D reconstructions (**f**), and calculated volumes of subcutaneous fat (**g**) and visceral fat (**h**) from mice at week 15; $n = 6$ per group. **i**-**m**, The morphology (**i**), cell number (**j**, **l**) and area (**k**, **m**) of BAT and liver tissue at week 15; $n = 4$ per group. n-u, The weights of subcutaneous white adipose tissue (**n**) and epididymal white adipose tissue (**o**) and serum triglyceride (**p**), total cholesterol (**q**), low-density lipoprotein cholesterol (**r**), and high-density lipoprotein cholesterol (**s**) levels. the relative triglyceride content in the liver (**t**), and the relative triglyceride content in epididymal white adipose tissue (**u**) at week 15. $n = 5$ per group. The data are presented as the mean ± s.e.m. #$P < 0.05$, ##$P < 0.01$, ###$P < 0.001$, ####$P < 0.0001$ vs. the ND group; *$P < 0.05$, **$P < 0.01$, ***$P < 0.001$ vs. the cycHFD group

disorders, including hyperglycemia, dyslipidemia, and tissue steatosis, in mice re-exposed to a HFD.

Increased energy expenditure and changes in serum factor levels

Resting energy expenditure and adaptive thermogenesis have been proposed to play a role in postdieting weight regain [19]. Therefore, we investigated whether FMT intervention could affect metabolic parameters. Indeed, compared to the cycHFD group, the FMT-C groups exhibited significantly increased oxygen consumption (Fig. 3a, b) and energy expenditure (Fig. 3c, d) without an increase in food intake (Fig. 3e). Given the crucial role of UCP1 in adipose thermogenesis [20], we analyzed UCP1 expression in BAT from both the FMT-C and cycHFD groups. UCP1 expression was significantly upregulated in the FMT-C groups compared to the cycHFD group (Fig. 3g, h).

IL-6 and TNF-α are two important pro-inflammatory factors found in serum. Serum levels of IL-6 (Fig. 3i) and TNF-α (Fig. 3j) were lower in the FMT-C groups than in the cycHFD group.

Leptin and adiponectin are hormone-like proteins secreted mainly by white adipose tissue, and they play critical roles in regulating food intake, body weight, energy expenditure, and neuroendocrine function [21, 22]. Similarly, compared to the cycHFD group, serum leptin levels in the FMT-C groups were significantly lower (Fig. 3k), while adiponectin levels were higher (Fig. 3l) in the FMT-C group than in the cycHFD group. Collectively, these data clearly demonstrate that FMT modulates energy homeostasis, immune homeostasis, and adipose tissue function in mice re-exposed to a HFD.

The regulatory effect of FMT on hepatic lipid metabolism

The liver plays a pivotal role in metabolism, particularly in lipid metabolism [23]. Therefore, we conducted untargeted lipidomic analysis to determine potential alterations in hepatic lipid metabolites among the FMT-C and cycHFD groups. In total, we detected 965 individual lipid species belonging to 24 classes of lipid metabolites. PCA

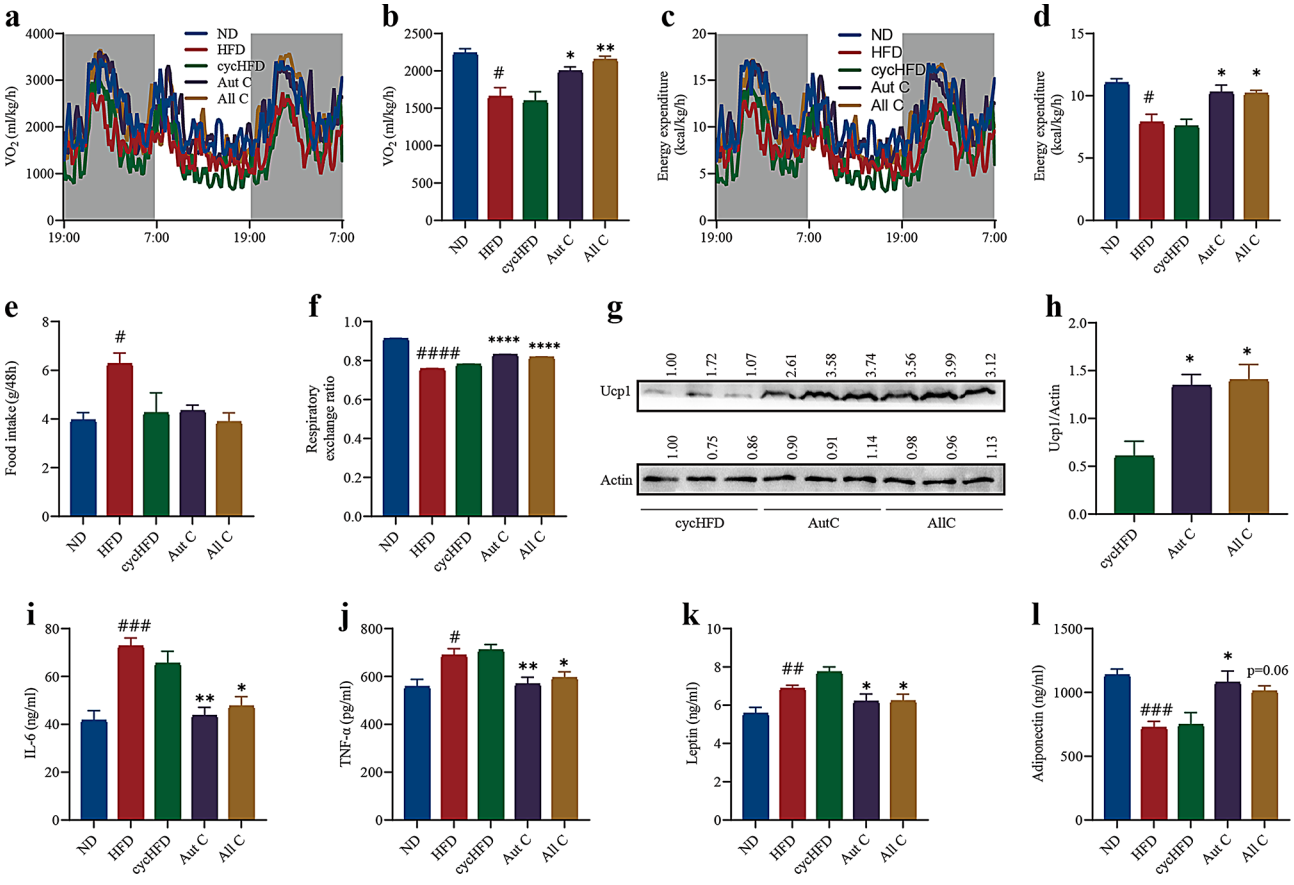

Fig. 3 Increased energy expenditure and changes in serum factor levels. **a**-**f**, O2 consumption (**a**, **b**), energy, expenditure (**c**, **d**), food intake (**e**) and the RER (**f**) over 36 h at week 15; $n = 3$ per group. **g**-**h**, Western blots for UCP1 in brown adipose tissue (**g**) and relative quantification of UCP1 at week 15; $n = 3$ per group. β-Actin served as the loading control Full-length blots are presented in Supplementary Fig. 1. **i**-**l**, The levels of serum IL-6 (**i**), TNF-a (**j**), leptin (**k**) and adiponectin (**l**) at week 15; $n = 6$ in each group. The data are presented as the mean ± s.e.m. #$P < 0.05$, ##$P < 0.01$, ###$P < 0.001$, ####$P < 0.0001$ vs. the ND group; *$P < 0.05$, **$P < 0.01$ vs. the cycHFD group

revealed marked differences in hepatic lipid metabolites between the FMT-C and cycHFD groups (Fig. 4a, b).

OPLS-DA was performed to identify significantly different metabolites. Clear spatial separations were observed between the AutC and cycHFD groups (Fig. 4c) and between the AllC and cycHFD groups (Fig. 4e). The reliability of the OPLS-DA models was validated by a permutation test, indicating that the models were not overfitting (Fig. 4d, f).

Lipid metabolites with an FDR < 0.05 and FC > 2.0 were considered differentially abundant between the groups. A total of 182 differentially abundant lipid species were identified between the AutC and cycHFD groups, which included 28 upregulated and 154 downregulated metabolites (Fig. 4g). Similarly, 203 differentially abundant lipid species were identified between the AllC and cycHFD groups, comprising 94 upregulated and 109 downregulated metabolites (Fig. 4i). The percentage plots (Fig. 4h, j) showed that TGs accounted for the largest proportion of the differential lipid species in both the AutC and AllC groups compared to the cycHFD group (68% and 74%, respectively). Based on the VIP score analysis (Fig. 4k, l), we further screened the top 40 differentially abundant lipid species for subsequent analyses, the results of which are detailed in Supplementary Table S1. Among these lipid species, TG (46:3/FA16:1), TG (48:4/FA16:1), TG (48:4/FA18:2), TG (50:5/FA18:2), TG (50:5/FA18:3), TG (56:9/FA20:5), TG 47:3 – 1, TG 49:4 – 2, TG 51:6 – 3, PC 37:1–1, PC 44:1, PC 44:4, PC O-36:3 – 1, and SM 39:2 were identified as common differentially abundant lipid species induced by allogeneic and autologous FMT. These shared differentially abundant metabolites may provide novel insights into the role of the liver in controlling post-dieting weight regain.

To further elucidate the biochemical processes associated with these common differentially abundant metabolites, we performed KEGG pathway enrichment analysis. These metabolites were implicated in 19 metabolic pathways (Fig. 4m), including thermogenesis, regulation of lipolysis in adipocytes, insulin resistance, fat digestion and absorption, vitamin digestion and absorption, cholesterol metabolism, lipid metabolism, and atherosclerosis. Most of these pathways are closely associated with glucose and lipid metabolism. Additionally, the expression of FASN was lower in the FMT-C groups than in the cycHFD group (Fig. 4n, o). These findings demonstrate that FMT inhibits hepatic lipid synthesis in mice re-exposed to a HFD.

Changes in the SCFA levels

To investigate the effect of FMT on intestinal SCFAs, we measured SCFA levels in the cecal contents from each group. Compared to the cycHFD group, the propionate levels in the FMT-C groups were significantly higher (Fig. 5b), while isobutyric acid levels showed a trend toward increase (Fig. 5c). Additionally, pentanoic acid levels also trended upward in the AllC group (Fig. 5f). However, no significant differences were found in acetic acid (Fig. 5a), butyric acid (Fig. 5d), or pentanoic acid (Fig. 5e) levels among these groups. Therefore, FMT primarily increased the levels of propionic acid in the regulation of SCFAs.

Alterations in the gut microbiota

The gut microbiota in the AutC, AllC, and cycHFD groups was analyzed through metagenomic sequencing, with taxonomic statistical analysis conducted at both the phylum and genus levels. At the phylum level, the abundances of Bacteroidetes and Firmicutes were similar between the AutC and cycHFD groups. However, in comparison to the cycHFD group, the AllC group exhibited a lower relative abundance of *Bacteroidetes* and a higher relative abundance of *Firmicutes*, resulting in an increased Firmicutes-to-Bacteroidetes ratio (Fig. 6a). At the genus level, *Clostridium* and *Desulfovibrio* were more abundant in the AutC group than in the cycHFD group, while *Candidatus Amulumruptor* and *Ileibacterium* were less abundant. Additionally, the AllC group had a higher abundance of *Bacteroides* and a lower abundance of *Mucispirillum* compared to the cycHFD group (Fig. 6b). Differences in microbial composition between the samples were assessed using β diversity analysis. Bray–Curtis-based PCoA revealed no clear spatial separation among the three groups (Fig. 6c, d). These results indicate that FMT induced changes in the microbiota within the FMT-C groups, but the overall microbial composition remained similar to that of the cycHFD group.

Linear discriminant analysis effect size (LEfSe) analysis was performed to identify key differences among the three groups at all taxonomic levels. With an LDA value of 2, the results revealed that *En*terorhabdus caecimuris (Fig. 6o) and *Enterorhabdus* (Fig. 6p) were commonly enriched in the FMT-C groups, while *Betaproteobacteria*, *Burkholderiales*, *Sutterellaceae*, *Bacteroides stercorirosoris*, *Turicimonas*, *Turicimonas muris*, *Acetivibrio*, and *Acetivibrio ethanolgignens* (Fig. 6g-n) were enriched in the cycHFD group.

Spearman correlation analysis was conducted to evaluate the relationships among three short-chain fatty acids (SCFAs), weight regain, and commonly altered bacteria. The results indicated that propionic acid levels were negatively correlated with the abundances of *Betaproteobacteria*, *Burkholderiales*, *Sutterellaceae*, and *Bacteroides stercorirosoris*, but positively correlated with the abundances of *Enterorhabdus caecimuris* and *Enterorhabdus*. Isobutyric acid levels showed a negative correlation with the abundances of *Betaproteobacteria*, *Burkholderiales*, *Sutterellaceae*, *Bacteroides stercorirosoris*, *Turicimonas*,

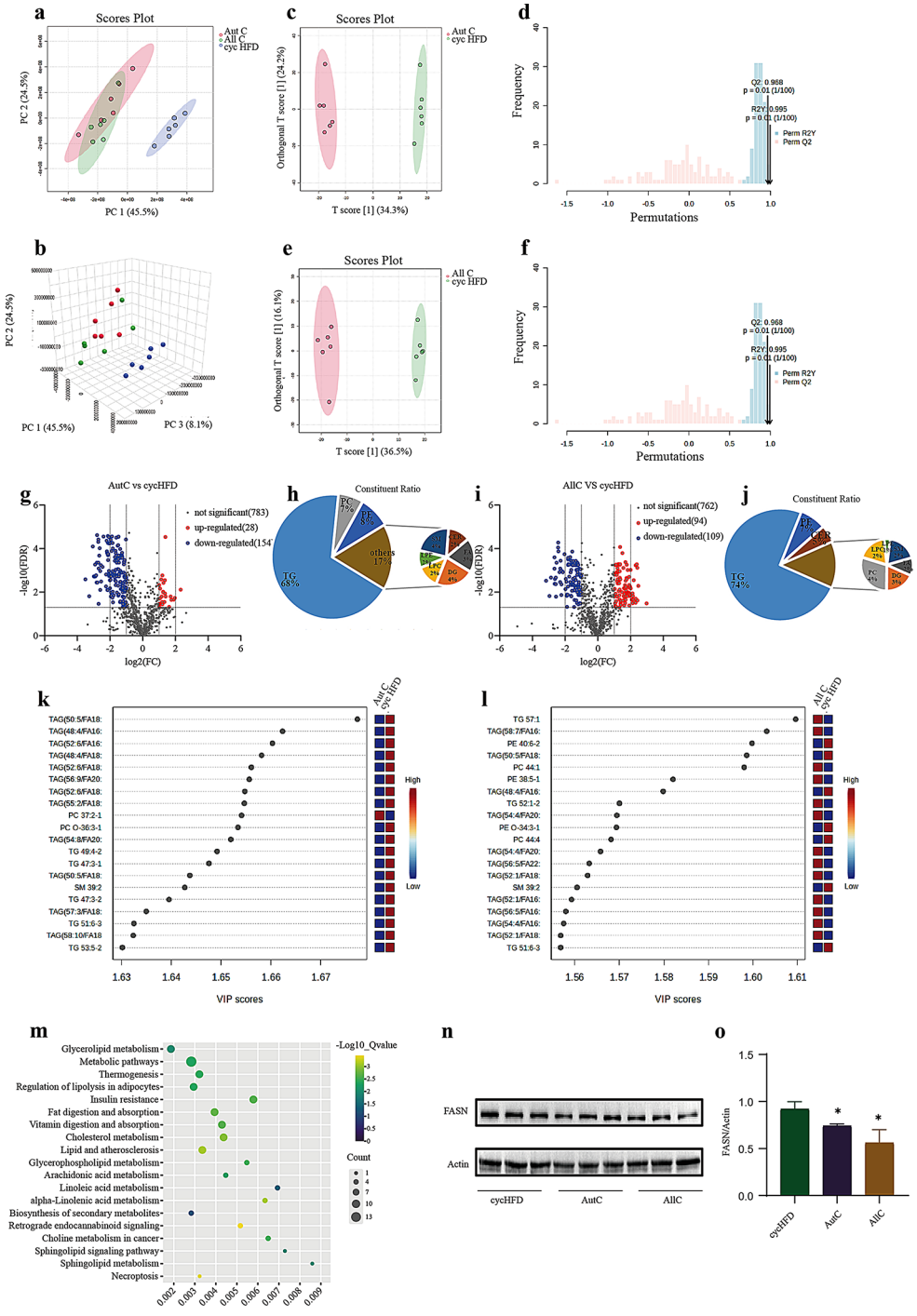

Fig. 4 The regulatory effect of FMT on hepatic lipid metabolism. **a**-**b**, Score plots (**a**) and 2D score plots (**b**) of PCA for discriminating the hepatic metabolome in mice from the AllC, AutC and cycHFD groups; $n = 6$ per group. c-d, An OPLS-DA score plot (**c**) and one hundred permutations (**d**) were generated and plotted for the AutC and cycHFD groups; $n = 6$ per group. e-f, An OPLS-DA score plot (**e**) and one hundred permutations (**f**) were generated and plotted for the AllC and cycHFD groups; $n = 6$ per group. **g**-**h**, Differential lipid metabolites between the AutC and cycHFD groups are shown in a volcano plot (**g**), and the respective composition ratios are shown in a pie chart (**h**). $n = 6$ per group. **i**-**j**, Differential lipid metabolites between the AllC and cycHFD groups (**i**) and the respective composition ratio (**j**). $n = 6$ per group. **k**-**l**, Top 20 VIP scores between the AutC and cycHFD groups (**k**) and between the AllC and cycHFD groups (**l**). **m**, Metabolic pathway enrichment analyses of differentially abundant metabolites. **n**-**o**, Western blots for FASN in liver tissue (**n**), and relative quantification of FASN at week 15; $n = 3$ per group. β-Actin served as the loading control. Full-length blots are presented in Supplementary Fig. 1. The data are presented as the mean ± s.e.m. $^{*}P < 0.05$, $^{**}P < 0.01$ vs. the cycHFD group

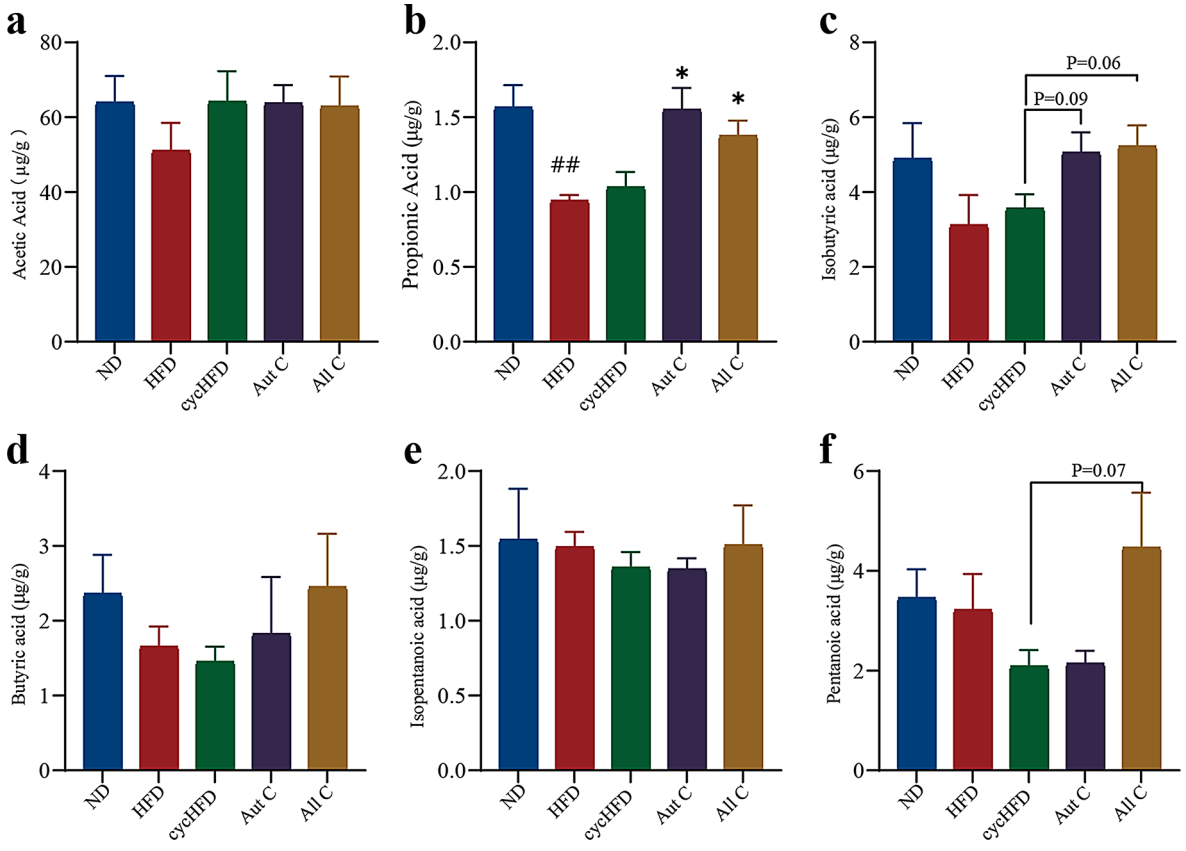

Fig. 5 Changes in the SCFA levels. **a**-**f**, The levels of acetic acid (**a**), propionic acid (**b**), isobutyric acid (**c**), butyric acid (**d**), isopentanoic acid (**e**), and pentanoic acid (**f**) in the cecal contents at week 15. $n = 5$ per group. The data are presented as the mean ± s.e.m. ##$P < 0.01$ vs. the ND group; *$P < 0.05$ vs. the cycHFD group

and Turicimonas muris, but a positive correlation with *Enterorhabdus caecimuris* and *Enterorhabdus* abundances. However, no significant correlation was found between pentanoic acid and these commonly altered bacteria. Furthermore, weight regain exhibited a negative correlation with the abundances of *Enterorhabdus caecimuris* and *Enterorhabdus*, but a positive correlation with the abundances of *Sutterellaceae*, *Bacteroides stercorirosoris*, *Turicimonas*, and *Turicimonas muris*. Collectively, these data suggest that changes in gut microbiota composition induced by FMT are associated with propionic acid levels and weight regain.

Discussion

In this study, both autologous and allogeneic fecal effectively reduced weight regain, adipogenesis, and hepatic steatosis in mice exposed to obesity-promoting conditions. Furthermore, FMT interventions inhibited the elevation of serum fasting insulin, triglycerides and total cholesterol and alleviated glucose intolerance and insulin resistance. These findings suggest that both autologous and allogeneic FMTs hold potential as interventions for preventing weight regain following dieting. However, body weight was not influenced by FMT during the initial high-fat or normal feeding periods, indicating that dietary changes significantly impacted the weight cycle, and that early intervention with FMT did not prevent post-dieting weight regain. Therefore, our focus shifted toward analyzing the common changes induced by autologous and allogeneic FMTs in mice re-exposed to a HFD for further mechanistic investigation.

During the process of weight loss and subsequent weight regain, both the proportion and function of immune cells are altered, leading to changes in the secretion of pro-inflammatory cytokines such as (IL-1), IL-6, and tumor necrosis factor (TNF) [24–26]. Chronic inflammation may play a crucial role in regulating the development of obesity and metabolic syndrome. Inflammatory factors have also been implicated in influencing adipocyte thermogenesis and energy expenditure [27]. In this study, serum levels of IL-6 and TNF-α were lower in the FMT-C groups than in the cycHFD group. Given the interaction between serum components and adipose tissue, systemic inflammation may affect various functions of adipose tissue, including lipid synthesis, adipokine secretion, and adipocyte thermogenesis. Indeed, our findings showed greater energy expenditure, oxygen consumption, and uncoupling expression in the FMT-C

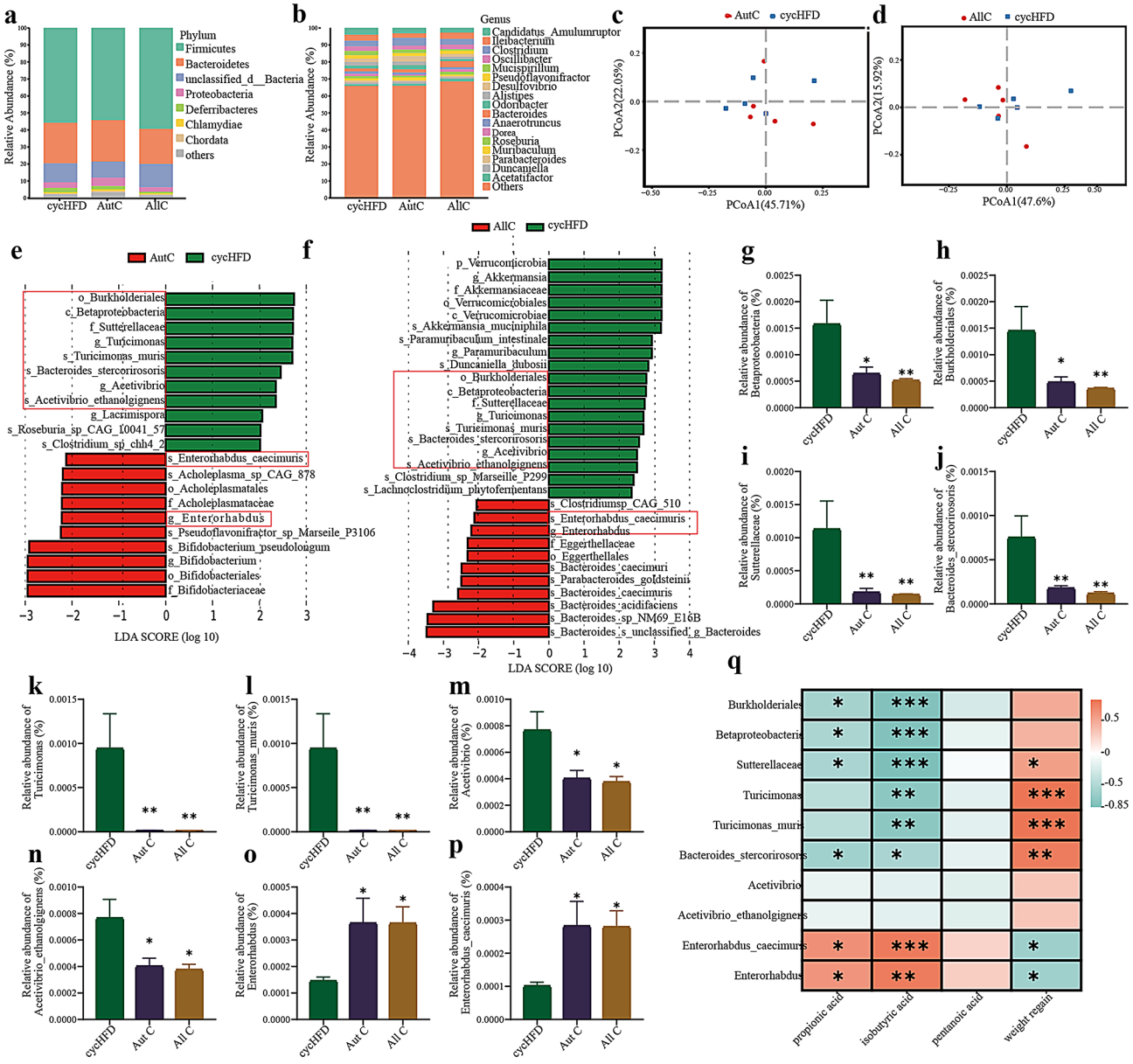

Fig. 6 Alterations in the gut microbiota. the phylum and genus levels. **a**-**b**, Relative abundances of the gut microbiota at the phylum level (**a**) and genus level (**b**). **c**-**d**, PCoA of the microbiota composition in the AutC and cycHFD groups (**c**) and in the AllC and cycHFD groups (**d**). **e**-**f**, Distribution histogram based on the LDA of the AutC and cycHFD groups (**e**) and the AllC and cycHFD groups (**f**). **g**-**q**, The relative abundances of Betaproteobacteria (**g**), Burkholderiales (**h**), Sutterellaceae (**i**), Bacteroides stercorirosoris (**j**), Turicimonas (**k**), Turicimonas_muris (**l**), Acetivibrio (**m**), Acetivibrio_ethanolgignens (**n**), Enterorhabdus_caecimuris (**o**), and Enterorhabdus (**p**). **q**, Heatmap of correlations between the gut microbiota, SCFAs and weight regain in the AutC, AllC and cycHFD groups. $n = 5$ per group. The data are presented as the mean ± s.e.m. $^{*}P < 0.05$, $^{**}P < 0.01$, $^{***}P < 0.001$ vs. the cycHFD group

groups compared to the cycHFD group, which may contribute to reductions in weight regain and alleviation of related disorders.

Leptin and adiponectin are endocrine factors synthesized and released by adipose tissue. Serum leptin concentration is proportional to the size of adipose tissue [28]. Adiponectin has been demonstrated to possess insulin-sensitizing [29], anti-atherogenic and anti-inflammatory properties [30]. Our results showed a decrease in leptin levels and an increase in adiponectin levels in the FMT-C groups compared to the cycHFD group, indicating improved functionality of adipose tissue in the FMT-C groups.

SCFAs primarily consist of acetic acid, propionic acid, isobutyric acid, butyric acid, isopentanoic acid, and pentanoic acid. These short-chain fatty acids are major metabolites produced predominantly by gut microbiota in the colon during the fermentation of indigestible polysaccharides or fibers [31]. SCFAs contribute to maintaining mucosal homeostasis by enhancing gut

epithelial integrity and reducing the expression of numerous inflammatory cytokines [32]. It has been extensively documented that plasma and fecal SCFAs are associated with energy metabolism [33] and inflammation [34]. Previous studies have reported that propionic acid can decrease fatty acid levels in the liver and plasma, exert immunosuppressive effects, and potentially enhance tissue insulin sensitivity [35]. Similarly, this study found a significant increase in fecal propionic acid levels in the FMT-C groups, with a trend toward increased levels of isobutyric and pentanoic acids.

SCFAs are considered regulatory factors linking the gut and liver, as they can be absorbed in the colon and transported to the liver, where they regulate lipid metabolism [36]. Additionally, prior studies have shown that SCFAs can shift hepatic lipid metabolism from lipogenesis to fat oxidation via PPARγ-dependent signaling [37]. Lipidomic analysis revealed significant changes in hepatic lipid metabolism in the FMT-C groups, the largest proportion of differentially abundant metabolites. KEGG metabolic pathway and enrichment analyses indicated that TGs are involved in several critical metabolic pathways, including lipid and atherosclerosis, cholesterol metabolism, fat digestion and absorption, regulation of lipolysis in adipocytes, and thermogenesis. Moreover, FASN, a key metabolic enzyme involved in hepatic de novo lipogenesis, was downregulated in the livers of mice in the FMT-C groups. These findings demonstrate that increased SCFA levels trigger responses in hepatic lipid metabolism, contributing to the inhibition of post-dieting weight regain.

The results of the gut microbiota analysis revealed that the microbial composition of the FMT-C groups was similar to that of the cycHFD group, with several common changes observed in various low-abundance taxa. Our analysis demonstrated a greater abundance of several taxa, including Burkholderiales, Sutterellaceae, Turicimonas muris, Bacteroides stercorirosoris, and Acetivibrio ethanolgignens, in the cycHFD group compared to the FMT-C groups. In contrast, Enterorhabdus caecimuris was more abundant in the FMT-C groups. Correlation analysis results suggest that these commonly altered low-abundance bacteria may contribute to inhibiting post-dieting weight regain by influencing the production of short-chain or through other mechanisms. Interestingly, a randomized controlled human trial reported that alterations in low-abundance species played a crucial role in the effectiveness of FMT treatment for reducing weight regain [38]. Thus, the regulation of liver lipid metabolism by FMT may be linked to variations in the gut microbiome and increased levels of SCFAs.

Given the impact of antibiotic treatment on gut microbiota and body weight [39], no antibiotics were administered to the mice prior to FMT in this study, which may explain our findings from the gut microbiota analysis. We propose that propionic acid plays a crucial role in the interaction between the gut microbiota and liver metabolism during weight cycling, warranting further investigation in future research endeavors.

Limitation

From an innovation standpoint, while research on the gut-liver axis has yielded some results, there are limitations to this research. For example, antibiotics were not used prior to FMT transplantation, and the study did not verify whether the bacteria from FMT successfully colonized. Additionally, the preparation of one bacterium in this study was performed under aerobic conditions, which may adversely affect oxygen-sensitive bacteria, such as obligate anaerobes, a major component of the mouse gut microbiota. Future studies could focus on developing new FMT preparation methods to minimize adverse effects on the gut microbiota.

Conclusion

In conclusion, the results of this study demonstrate that FMT can mitigate post-diet weight regain by regulating hepatic lipid metabolism through the modulation of gut microbiota and SCFA production. These findings suggest that the gut-liver axis may have significant implications for addressing weight regain after both autologous and allogeneic FMT.

Abbreviations

FMT	ecal microbiota transplantation
HFD	high-fat diet
ND	normal diet
PBS	phosphate-buffered saline
TG	triglyceride
TC	total cholesterol
LDL-C	low-density lipoprotein cholesterol
HDL-C	high-density lipoprotein cholesterol
H&E	hematoxylin-eosin
BAT	brown adipose tissue
UCP1	uncoupling protein 1
FASN	fatty acid synthase
UHPLC-MS	Ultrahigh-performance liquid chromatography tandem mass spectrometry
GC–MS	Gas chromatography tandem mass spectrometry
SCFAs	short-chain fatty acids
ANOVA	one-way analysis of variance
PcoA	principal coordinates analysis
FPG	fasting plasma glucose
LefSe	Linear discriminant analysis effect size
TNF	tumor necrosis factor

Supplementary Information

The online version contains supplementary material available at https://doi.org/10.1186/s12866-025-03853-4.

Supplementary Material 1

Acknowledgements

We thank the staff of the Laboratory Animal Centre of Jiangnan University School of Medicine for the daily care of the animals.

Author contributions
Conceptualization, Dan Li, Jiai Yan and Hong Cao; methodology, Jiangwei Xu, Han Wang, Wanya Yi and Dandan Yang; validation and formal analysis, Ju Yang, Jing Sun and Yingyu Wang; investigation, Dan Li, Jiai Yan and Hong Cao; resources and data curation, Jiangwei Xu, Han Wang and Dan Li; writing—original draft preparation, Hong Cao, Han Wang and Jiangwei Xu; writing—review and editing, Dan Li, Jiai Yan, Jiangwei Xu, Han Wang and Hong Cao; visualization, Jiangwei Xu, Han Wang, Wanya Yi and Dandan Yang; supervision, Dan Li and Feng Zhang; project administration, Dan Li and Hong Cao; Funding acquisition, Hong Cao, Ju Yang, Jing Sun, Yingyu Wang, Feng Zhang, Jiai Yan and Dan Li. All authors have read and agreed to the published version of the manuscript.

Funding
This research was funded by National Key Research and Development Program of China (2023YFF1104305; 2022YFF1100601); National Natural Science Foundation of China (32101033; 82370809); Natural Science Foundation of Jiangsu Province (BK20210060; BK20210468); Key Research project of Health Commission of Jiangsu Province (K2023004; M2021055); Wuxi Science and Technology Bureau, "Taihu Light" Science and Technology Research program (Y202100; K202210261); Key discipline construction program of Wuxi Commission of Health (CXTD2021003); "Shuangbai Talents" research program of Wuxi Commission of Health (HB2023061; HB2023062; HB2023063); Clinical Research and translational medicine research program of Affiliated Hospital of Jiangnan University (LCYJ202303; LCYJ202347; LCYJ202322; LCYJ202310); Medical research projects in research-oriented hospitals of Affiliated Hospital of Jiangnan University (YJZ202305); Soft Science Project of Wuxi Science and Technology Association (to KX-23-B050; KX-23-C196).

Data availability
The datasets generated and/or analysed during the current study are available in the NCBI database [PRJNA1184324; https://www.ncbi.nlm.nih.gov/bioproject/PRJNA1184324].

Declarations

Ethical approval
The study protocol was approved by the Medical Ethics Committee of Jiangnan University (Ethical Review Number: JN.No20210615c0631115; Date:20210615).

Consent for publication
Not applicable.

Competing interests
The authors declare no competing interests.

Received: 2 October 2024 / Accepted: 28 February 2025
Published online: 13 March 2025

References

1. Nussbaumerova B, Rosolova H. Obesity and dyslipidemia. Curr Atheroscler Rep. 2023;25(12):947–55. https://doi.org/10.1007/s11883-023-01167-2.
2. Chen K, Shen Z, Gu W, Lyu Z, Qi X, Mu Y, et al. Prevalence of obesity and associated complications in China: A cross-sectional, real-world study in 15.8 million adults. Diabetes Obes Metab. 2023;25(11):3390–9. https://doi.org/10.1111/dom.15238.
3. Krzysztoszek J, Laudańska-Krzemińska I, Bronikowski M. Assessment of epidemiological obesity among adults in EU countries. Ann Agric Environ Med. 2019;26(2):341–9. https://doi.org/10.26444/aaem/97226.
4. Blüher M. Obesity: global epidemiology and pathogenesis. Nat Rev Endocrinol. 2019;15(5):288–98. https://doi.org/10.1038/s41574-019-0176-8.
5. Alegría Ezquerra E, Castellano Vázquez JM, Alegría Barrero A. [Obesity, metabolic syndrome and diabetes: cardiovascular implications and therapy]. Rev Esp Cardiol. 2008;61(7):752–64.
6. Aronne LJ, Hall KD, Leibel JMJ, Lowe RL, Rosenbaum MR. Describing the Weight-Reduced State: physiology, behavior, and interventions. Obes (Silver Spring). 2021;29(Suppl 1):S9–24. https://doi.org/10.1002/oby.23086.
7. Pietiläinen KH, Saarni SE, Kaprio J, Rissanen A. Does dieting make you fat? A twin study. Int J Obes (Lond). 2012;36(3):456–64. https://doi.org/10.1038/ijo.2011.160.
8. Dulloo AG, Jacquet J, Montani JP, Schutz Y. How dieting makes the lean fatter: from a perspective of body composition autoregulation through adipostats and proteinstats awaiting discovery. Obes Rev. 2015;16(Suppl 1):25–35. https://doi.org/10.1111/obr.12253.
9. Cani PD. Microbiota and metabolites in metabolic diseases. Nat Rev Endocrinol. 2019;15(2):69–70. https://doi.org/10.1038/s41574-018-0143-9.
10. Liu R, Hong J, Xu X, Feng Q, Zhang D, Gu Y, et al. Gut Microbiome and serum metabolome alterations in obesity and after weight-loss intervention. Nat Med. 2017;23(7):859–68. https://doi.org/10.1038/nm.4358.
11. David LA, Maurice CF, Carmody RN, Gootenberg DB, Button JE, Wolfe BE, et al. Diet rapidly and reproducibly alters the human gut Microbiome. Nature. 2014;505(7484):559–63. https://doi.org/10.1038/nature12820.
12. Martinez-Guryn K, Hubert N, Frazier K, Urlass S, Musch MW, Ojeda P, et al. Small intestine microbiota regulate host digestive and absorptive adaptive responses to dietary lipids. Cell Host Microbe. 2018;23(4):458–e695. https://doi.org/10.1016/j.chom.2018.03.011.
13. Aron-Wisnewsky J, Clément K, Nieuwdorp M. Fecal microbiota transplantation: a future therapeutic option for obesity/diabetes?? Curr Diab Rep. 2019;19(8):51. https://doi.org/10.1007/s11892-019-1180-z.
14. Thaiss CA, Itav S, Rothschild D, Meijer MT, Levy M, Moresi C, et al. Persistent Microbiome alterations modulate the rate of post-dieting weight regain. Nature. 2016;540(7634):544–51. https://doi.org/10.1038/nature20796.
15. Chang CJ, Lin CS, Lu CC, Martel J, Ko YF, Ojcius DM, et al. Ganoderma lucidum reduces obesity in mice by modulating the composition of the gut microbiota. Nat Commun. 2015;6:7489. https://doi.org/10.1038/ncomms8489.
16. Yang K, Cheng H, Gross RW, Han X. Automated lipid identification and quantification by multidimensional mass spectrometry-based shotgun lipidomics. Anal Chem. 2009;81(11):4356–68. https://doi.org/10.1021/ac900241u.
17. Fu L, Niu B, Zhu Z, Wu S, Li W. CD-HIT: accelerated for clustering the next-generation sequencing data. Bioinformatics. 2012;28(23):3150–2. https://doi.org/10.1093/bioinformatics/bts565.
18. Peng Y, Leung HC, Yiu SM, Chin FY. Bioinformatics. 2012;28(11):1420–8. https://doi.org/10.1093/bioinformatics/bts174. IDBA-UD: a de novo assembler for single-cell and metagenomic sequencing data with highly uneven depth.
19. Presby DM, Rudolph MC, Sherk VD, Jackman MR, Foright RM, Jones KL, et al. Lipoprotein lipase overexpression in skeletal muscle attenuates weight regain by potentiating energy expenditure. Diabetes. 2021;70(4):867–77. https://doi.org/10.2337/db20-0763.
20. Nicholls DG. The Hunt for the molecular mechanism of brown fat thermogenesis. Biochimie. 2017;134:9–18. https://doi.org/10.1016/j.biochi.2016.09.003.
21. Perks KL, Ferreira N, Richman TR, Ermer JA, Kuznetsova I, Shearwood AJ, et al. Adult-onset obesity is triggered by impaired mitochondrial gene expression. Sci Adv. 2017;3(8):e1700677. https://doi.org/10.1126/sciadv.1700677.
22. Greer KB, Falk GW, Bednarchik B, Li L, Chak A. Associations of serum adiponectin and leptin with Barrett's esophagus. Clin Gastroenterol Hepatol. 2015;13(13):2265–72. https://doi.org/10.1016/j.cgh.2015.02.037.
23. Mitani S, Takayama K, Nagamoto Y, Imagawa K, Sakurai F, Tachibana M, et al. Human ESC/iPSC-Derived Hepatocyte-like cells achieve Zone-Specific hepatic properties by modulation of WNT signaling. Mol Ther. 2017;25(6):1420–33. https://doi.org/10.1016/j.ymthe.2017.04.006.
24. Cottam MA, Caslin HL, Winn NC, Hasty AH. Multiomics reveals persistence of obesity-associated immune cell phenotypes in adipose tissue during weight loss and weight regain in mice. Nat Commun. 2022;13(1):2950. https://doi.org/10.1038/s41467-022-30646-4.
25. Caslin HL, Bhanot M, Bolus WR, Hasty AH. Adipose tissue macrophages: unique polarization and bioenergetics in obesity. Immunol Rev. 2020;295(1):101–13. https://doi.org/10.1111/imr.12853.
26. Zeyda M, Farmer D, Todoric J, Aszmann O, Speiser M, Györi G, et al. Human adipose tissue macrophages are of an anti-inflammatory phenotype but capable of excessive pro-inflammatory mediator production. Int J Obes (Lond). 2007;31(9):1420–8. https://doi.org/10.1038/sj.ijo.0803632.
27. Reilly SM, Saltiel AR. Adapting to obesity with adipose tissue inflammation. Nat Rev Endocrinol. 2017;13(11):633–43. https://doi.org/10.1038/nrendo.2017.90.
28. Friedman JM, Halaas JL. Leptin and the regulation of body weight in mammals. Nature. 1998;395(6704):763–70. https://doi.org/10.1038/27376.
29. Yamauchi T, Kamon J, Waki H, Terauchi Y, Kubota N, Hara K, et al. The fat-derived hormone adiponectin reverses insulin resistance associated with

both lipoatrophy and obesity. Nat Med. 2001;7(8):941–6. https://doi.org/10.1038/90984.
30. Okamoto Y, Kihara S, Ouchi N, Nishida M, Arita Y, Kumada M, et al. Adiponectin reduces atherosclerosis in Apolipoprotein E-deficient mice. Circulation. 2002;106(22):2767–70. https://doi.org/10.1161/01.cir.0000042707.50032.19.
31. Cummings JH, Pomare EW, Branch WJ, Naylor CP, Macfarlane GT. Short chain fatty acids in human large intestine, portal, hepatic and venous blood. Gut. 1987;28(10):1221–7. https://doi.org/10.1136/gut.28.10.1221.
32. Tan JK, Macia L, Mackay CR. Dietary fiber and SCFAs in the regulation of mucosal immunity. J Allergy Clin Immunol. 2023;151(2):361–70. https://doi.org/10.1016/j.jaci.2022.11.007.
33. Hu J, Lin S, Zheng B, Cheung PCK. Short-chain fatty acids in control of energy metabolism. Crit Rev Food Sci Nutr. 2018;58(8):1243–9. https://doi.org/10.1080/10408398.2016.1245650.
34. Jiang K, Wang D, Su L, Liu X, Yue Q, Li B, et al. Structural characteristics of locust bean gum hydrolysate and its alleviating effect on dextran sulfate sodium-induced colitis. Front Microbiol. 2022;13:985725. https://doi.org/10.3389/fmicb.2022.985725.
35. Al-Lahham SH, Peppelenbosch MP, Roelofsen H, Vonk RJ, Venema K. Biological effects of propionic acid in humans; metabolism, potential applications and underlying mechanisms. Biochim Biophys Acta. 2010;1801(11):1175–83. https://doi.org/10.1016/j.bbalip.2010.07.007.
36. den Besten G, Gerding A, van Dijk TH, Ciapaite J, Bleeker A, van Eunen K, et al. Protection against the metabolic syndrome by Guar Gum-Derived Short-Chain fatty acids depends on peroxisome Proliferator-Activated receptor γ and Glucagon-Like Peptide-1. PLoS ONE. 2015;10(8):e0136364. https://doi.org/10.1371/journal.pone.0136364.
37. den Besten G, Bleeker A, Gerding A, van Eunen K, Havinga R, van Dijk TH, et al. Short-Chain fatty acids protect against High-Fat Diet-Induced obesity via a PPARγ-Dependent switch from lipogenesis to fat oxidation. Diabetes. 2015;64(7):2398–408. https://doi.org/10.2337/db14-1213.
38. Kamer O, Rinott E, Tsaban G, Kaplan A, Yaskolka Meir A, Zelicha H, et al. Successful weight regain Attenuation by autologous fecal microbiota transplantation is associated with non-core gut microbiota changes during weight loss; randomized controlled trial. Gut Microbes. 2023;15(2):2264457. https://doi.org/10.1080/19490976.2023.2264457.
39. Bongers KS, McDonald RA, Winner KM, Falkowski NR, Brown CA, Baker JM, et al. Antibiotics cause metabolic changes in mice primarily through Microbiome modulation rather than behavioral changes. PLoS ONE. 2022;17(3):e0265023. https://doi.org/10.1371/journal.pone.0265023.

Publisher's note

Springer Nature remains neutral with regard to jurisdictional claims in published maps and institutional affiliations.